

ISTITUTO NAZIONALE DI FISICA NUCLEARE

Sezione di Milano

INFN/TC-90/21
29 Ottobre 1990

P. Pierini, W.M. Fawley, W.M. Sharp:

**MULTIDIMENSIONAL SIMULATIONS OF THE ELFA SUPERRADIANT
FREE-ELECTRON LASER**

Work presented to the
12th International FEL Conference
Paris, September 17-21, 1990

Servizio Documentazione
dei Laboratori Nazionali di Frascati

MULTIDIMENSIONAL SIMULATIONS OF THE ELFA SUPERRADIANT FREE-ELECTRON LASER*

P. Pierini
INFN - Sezione di Milano, Via Celoria 16, 20133 Milano, Italy

W.M. Fawley
Lawrence Berkeley Laboratory, Berkeley, CA 94720 USA

W.M. Sharp
INFN - Sezione di Milano, Via Celoria 16, 20133 Milano, Italy
Permanent address: Lawrence Livermore National Laboratory, Livermore, California 94550

ABSTRACT

ELFA (Electron Laser Facility for Acceleration) is a high-gain, microwave ($\nu = 100$ GHz) free-electron laser (FEL) facility driven by an rf-linac. ELFA will test the existence of the theoretically predicted regimes of strong and weak superradiance. Both regimes can be studied with the same FEL by changing the height of the interaction waveguide, which controls the radiation group velocity, and thus the relative slippage between electrons and photons.

The operation of ELFA has been modeled using a modified version of the two-dimensional, time-dependent sideband code GINGER. The simulations take into account the time and space variations of the radiation field, as well as the space charge and transverse emittance of the electron beam. The sensitivity of the superradiant signal to variations of the beam emittance, energy and energy spread is examined.

1. - INTRODUCTION

ELFA is an INFN-funded rf linac-driven microwave free-electron laser (FEL) project. One of its goals is the experimental test of the analytically¹ and numerically² predicted regimes of cooperative spontaneous emission, namely the superradiant regimes, where the emitted power scales as the square of the electron density, and hence of the current. ELFA³ will operate at the

* This work was partially supported by the Director, Office of Energy Research, Office of Basic Energy Sciences, Advanced Energy Projects Division, U.S. Dept. of Energy under Contract No. DE-AC03-76SF00098.

frequency of 100 GHz, employing a 6-cm long, 10-20-MeV and 400-A electron beam. With this choice of parameters, slippage effects and superradiance play an important role in the FEL physics. ELFA, with a single experimental apparatus, and three different waveguide configurations, will have the possibility of exploring the three dynamical regimes of a FEL: the already observed steady state regime and the two novel regimes of weak and strong superradiance⁴.

These regimes were the object of several 1-D numerical studies (see e.g, ^{4,5})m both for the case of free space and waveguide propagation. These models, however, do not take into account the transverse structure of the electron beam, and cannot describe the effect of beam emittance on the radiated power, nor the competition between the different waveguide modes. Consequently, we have modified a microwave version of the 2-D time-dependent sideband code GINGER⁶ to take into account the proper boundary conditions of the transit time problem, necessary here to model effectively the dynamical behavior of the short electron bunches provided by the electron linac. We have done extensive GINGER simulations to simulate three waveguide configurations, in order to predict ELFA main features in each different case. We have then studied the effect of beam emittance on the radiated power. A description of the result is presented here.

Table I summarizes the overall parameters used in the simulations.

Table I. Parameters used for GINGER ELFA simulations

| | | |
|--------------------------------|--------------|-----------------------|
| Wiggler period | λ_w | 12 cm |
| Wiggler length | L_w | 6 m |
| Wiggler rms parameter | a_w | 3 |
| Wiggler focussing factors | k_y, k_x | $k_w/2$ |
| Beam Lorentz factor | γ | 10-20 |
| Radiation frequency | ν | 100 GHz |
| Waveguide width | a | 5 cm |
| Waveguide height | b | 1-3 cm |
| Beam hard edge norm. emittance | ϵ_n | 0.05-1.0 π cm-rad |
| Beam current | I | 400 A |
| Beam length L_b | δ | cm |
| Fundamental FEL parameter | ρ | 0.02-0.04 |
| Signal input power | P_{in} | 20 W |

2. - ELFA WAVEGUIDES

In many FEL's such as those driven by long pulse induction linacs, slippage effects are negligible because the e-beam length L_b (meters) is much greater than the slippage length L_s . However, in rf

linac-driven FEL's, the electron pulses are much shorter (e.g. 6 cm in ELFA) and the slippage length can be a significant fraction of L_b , especially at microwave wavelengths. Since L_s is proportional to $(v_g - v_{el})$, one can reduce or even suppress slippage when the FEL radiation propagates in a waveguide⁷. Here $v_g = c^2 k_{||} / \omega$ is the radiation group velocity, $v_{el} = \omega / (k_{||} + k_w)$ is the longitudinal electron velocity at FEL resonance, $k_{||}$ and ω are the radiation longitudinal wavenumber and angular frequency respectively. Use of the waveguide dispersion relation can show that slippage is entirely suppressed when $k_{\perp}^2 = k_w k_{||}$; for the TE₀₁ mode in ELFA with $k_{\perp} = \pi/b$, this is equivalent to b approximately equal to 0.95 cm. Thus, the three ELFA waveguides of 1.0, 1.2, and 3.0 cm (corresponding to resonant γ 's of 19.30, 17.28 and 14.76 respectively for a normalized vector potential of $a_w \cong 3$), permit exploration of a wide range of slippage length/beam length ratios.

The fundamental FEL parameter⁸ ρ in a waveguide is given by:

$$\rho = \frac{1}{\gamma} \left(\frac{a_w}{4} \frac{\omega_p}{ck_w + ck_{||} + \omega} f_b \right)^{2/3} \quad (1)$$

Here $\omega_p^2 = eJ/mc\epsilon_0$ is the plasma frequency, $J = I/(ab/2)$ is the effective current density inside the waveguide and f_b is the Bessel function difference for a linear wiggler. The parameter ρ gives the upper limit on the fractional energy spread for the classical high-gain instability⁸.

Table II displays ρ and the dimensionless parameters G , S , and K of ref. 4, for the ELFA waveguides. These parameters characterize the dynamical regime of a high-gain FEL. $G = 4\pi\rho N_w$ is the gain parameter defined where N_w is the number of wiggler periods; $S = L_s/L_b$ is the slippage parameter; and $K = S/G$ is the superradiant parameter. Strong superradiance phenomena requires $K \ll 1$, whereas weak superradiance can be observed when $S > 1$ and K is approximately 1. Strictly speaking, the pure steady state regime (i.e. no slippage effects) can be observed only when $S = 0$.

Table II. The gain and superradiant parameters for the three waveguides of the ELFA project

| b | ρ | G | S | K |
|-----|--------|------|------|-------|
| 1.0 | 0.039 | 24.5 | 0.22 | 0.009 |
| 1.2 | 0.035 | 22.0 | 0.92 | 0.042 |
| 3.0 | 0.025 | 15.7 | 2.25 | 0.143 |

3. - SIMULATION RESULTS: STEADY STATE EXPERIMENT ($b=1$ cm WAVEGUIDE)

In fig. 1 we show the time profile of the emitted radiation intensity at the end of the wiggler for the smaller waveguide. The time scale on this and the following plots is reversed and starts at the trailing edge of the radiation pulse. Since the slippage parameter is small ($S = 0.22$), the radiation pulse is only slightly lengthened from the initial electron beam length of 6 cm.

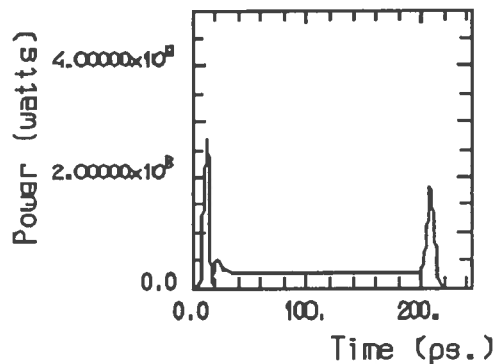


Fig. 1. 1 cm waveguide: time profile of the emitted radiation, the time scale is reversed and starts from the trailing edge of the radiation pulse. The beam emittance used in this simulation was 0.05π cm-rad.

The radiation intensity profile exhibits the typical shape of a strong superradiant (SR) spike in the trailing edge of the electron pulse, whereas a trace of the steady state (SS) high gain exponential growth along the wiggler is seen in the leading edge of the radiation pulse,^{2,4} escaping from the electron pulse. However, due to the small slippage distance, the SR spike reaches the same order of magnitude of the SS saturated power, namely 270 MW vs. 190 MW. The SR spike has nearly 85% of its power in the TE01 mode, 13% in the TE21 and less than 2% in the higher order modes. The spiking is confined to a very small region of the radiation pulse and contributes little to the average radiated power, as can be seen in fig. 2, where we plot the average power and its mode decomposition along the wiggler. This plot closely matches time-independent steady state simulations where slippage effects are ignored. In this sense, the $b=1$ cm waveguide configuration permits us to observe the steady state operation of ELFA with a very short bunch of electrons.

In fig. 3 we show the effect of increasing the electron beam's transverse emittance upon the spike power, the steady state saturated power and the average power. As we can see from the plot, a change of nearly an order of magnitude in the emittance leads to a significant decrease in the emitted power, both in the steady state instability and the superradiant spiking. This plot shows results only for those values of emittance for which the radiation field saturates before the end of

the 6-m wiggler. With higher values of emittance the superradiant trailing edge spiking can be still seen, reduced by many orders of magnitude in power but with a cleaner time shape.

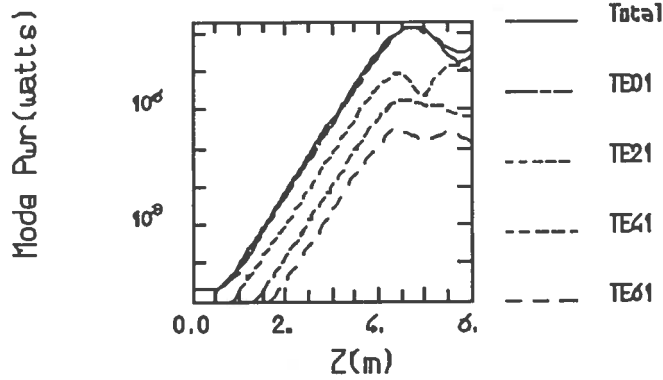


Fig. 2. 1 cm waveguide: average power in the radiation pulse as a function of the position in the wiggler, for the same case of fig. 1.

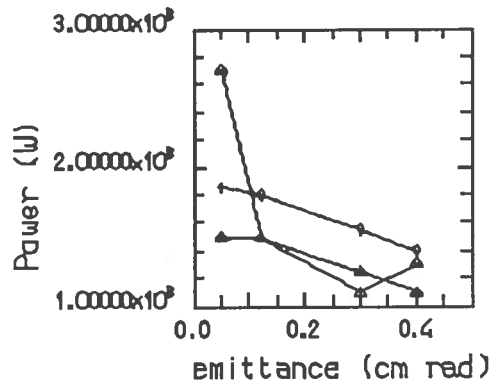


Fig. 3. 1 cm waveguide: we show the value of the superradiant spike (white triangles), of the steady state saturation peak (diamonds) and of the peak average power (black triangles), for four different values of the beam emittance.

The reduction in the SR spike and SS saturated power arises mainly from the larger emittance electron beam having a radius nearly equal to the waveguide height b , thus reducing the coupling between the beam and TE01 radiation field. A lesser effect is the increase in the effective fractional energy spread due to transverse emittance,

$$\eta \equiv \frac{\delta\gamma_{\parallel}}{\langle\gamma_{\parallel}\rangle} \approx \frac{k_w a_w}{4\sqrt{2}(1+a_w^2)} \epsilon_n \quad (2)$$

Here $\langle\gamma\rangle_{\parallel}$ and $\delta\gamma_{\parallel}$ are respectively the mean value and rms spread in the individual beam electrons' longitudinal Lorentz factors, and we have presumed curved pole tip focussing⁹. For ELFA parameters with $b = 1$ cm and $\epsilon_n = 0.4 \pi$ cm-rad, η is approximately 0.011 which is still small compared with FEL fundamental parameter $\rho = 0.039$.

4. - SIMULATION RESULTS: STRONG SUPERRADIANCE (b= 1.2-cm WAVEGUIDE)

In the ELFA 1.2-cm waveguide configuration, the superradiant spike has more time to interact with the electrons due to the increased slippage ($S = 0.92$). Figure 4 displays the time profile of the the calculated radiation intensity from a simulation with $\epsilon_n = 0.1 \pi$ cm-rad. The spike power reaches up to 440 MW and the steady state saturated power is 170 MW. Moreover, the average emitted power (fig. 5) is also increased due to the large area of the SR spike. As with the previous 1-cm waveguide case, an increase of the beam emittance of nearly an order of magnitude reduces the predicted output power (see fig. 6) due to the beam radius approaching b .

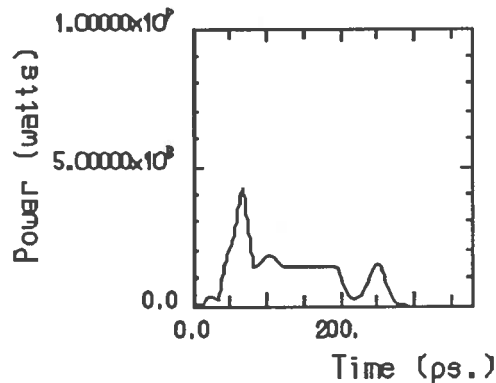


Fig. 4. As fig. 1, for the 1.2 cm waveguide and a beam emittance of 0.1π cm-rad.

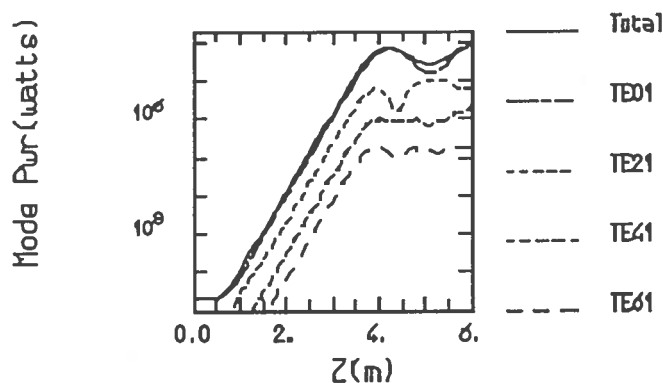


Fig. 5. As fig. 2, for the 1.2 cm waveguide case.

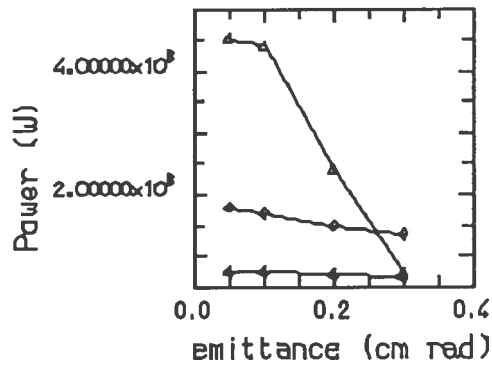


Fig. 6. As fig. 3, for the 1.2 cm waveguide case.

A number of simulations were done with non-zero instantaneous energy spreads keeping the emittance constant. The results showed that the SR spike remained present (albeit at reduced power) until $\Delta\gamma$ exceeded 0.7 (see fig. 7). This agrees with the energy spread criterion $\Delta\gamma < \gamma\rho$ approximately 0.60.

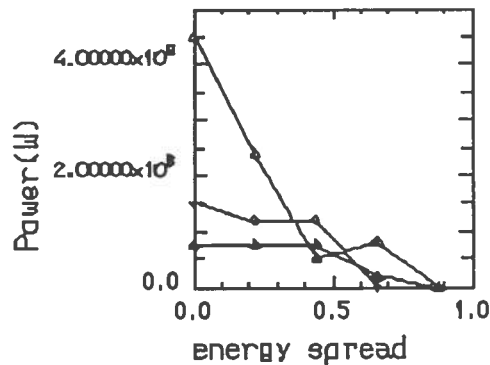


Fig. 7. Behavior of the superradiant spike (white triangles), the steady state saturation peak (diamonds), and the peak average power (black triangles) as a function of the absolute energy spread $\Delta\gamma$.

Figure 8 shows the same case presented in fig. 4, but with the wiggler field detuned 10% from resonance. In this case the steady state part of the radiation pulse does not exhibit any exponential growth, whereas the trailing edge SR spike is greatly enhanced, reaching nearly 1 GW of power. This off-resonant enhancement is a feature of superradiance previously predicted by 1-D analysis⁵.

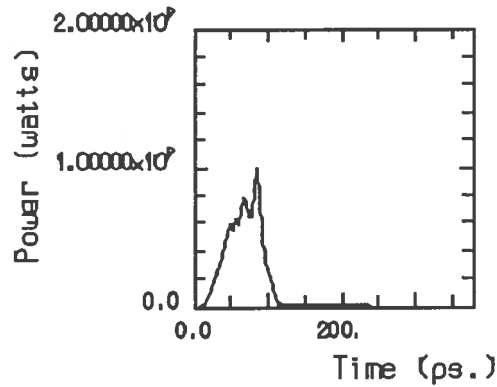


Fig. 8. Same parameters for fig. 4, but a 10% detuned wiggler field.

5. - SIMULATION RESULTS: WEAK SUPERRADIANCE ($b = 3$ -cm WAVEGUIDE)

With the 3-cm waveguide and ELFA parameters, we enter a completely different dynamical regime of a high-gain FEL, the weak superradiant regime, never observed experimentally. In this case the gain that a photon experiences in slipping through the electron pulse (given by K^{-1}) is smaller than in the previous cases, and the radiation escapes from the pulse before experiencing saturation⁴.

The predicted output radiation pulse (see fig.9) is both much longer in duration than the 200-ps electron beam pulse, due to the increased slippage ($S=2.22$), and exhibits a totally different temporal shape than the previous two cases. Now there is no flat (time-independent) part of the radiation pulse, denoting regions of stationary evolution, because $S > 1$.

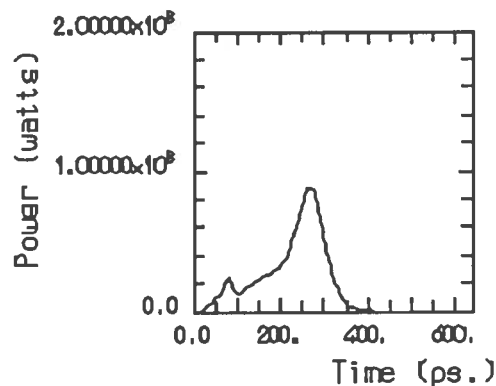


Fig. 9. 3 cm waveguide: time profile of the emitted radiation, for a beam emittance of 0.5π cm-rad.

In fig. 10 we plot the peak output power and the average power along the pulse as a function of emittance, with four values ranging from 0.05 to 0.5 π cm-rad. This variation of one order of magnitude in the beam transverse emittance results just in a 10% variation of the radiation power. Even with the 3X increase in beam size, there is still good coupling to the TE01 field of the large waveguide while the increase in effective fractional energy spread to 0.014 (see eq. 2) remains smaller than the corresponding FEL parameter $\rho = 0.025$.

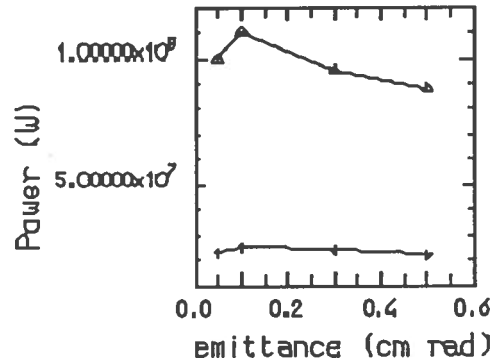


Fig. 10. 3 cm waveguide: peak superradiant power (triangles) and peak average power (diamonds) for four values of the beam emittance, ranging from 0.05 π cm-rad to 0.5 π cm-rad.

6. - CONCLUSIONS

The 2-D simulations results presented here show that both strong and weak superradiance should be clearly present in the ELFA experiment, in accord with previous 1-D work. There should not be difficulties with transverse mode competition nor with transverse beam emittances up to $\epsilon_n = 0.5 \pi$ cm-rad so long as the beam size remains a fraction of the waveguide height. Superradiance remains present for energy spreads up to $\Delta\gamma$ approximately equal to 0.5.

REFERENCES

- (1) R.Bonifacio, C.Maroli, N.Piovella, *Opt.Comm.*, **68**, (1988), 369;
- (2) R.Bonifacio, B.W.J.McNeil, *Nuclear Instr. and Meth.*, **A272**, (1988), 280;
- (3) R.Bonifacio et al., *Nucl. Instr. and Meth.*, **A289**, (1990), 1;
- (4) R.Bonifacio, B.W.J.McNeil, P.Pierini, *Phys. Rev. A*, **40**, (1989), 4467;
- (5) W.M.Sharp, W.M.Fawley, S.S.Yu, A.M.Sessler, R.Bonifacio and L.De Salvo Souza, *Nuclear Instr. and Meth.*, **A285**, (1989), 217;
- (6) R.A.Jong, W.M.Fawley, E.T.Scharlemann, *SPIE Vol. 1045 Modeling and Simulation of Laser Systems*, (1989), 18.
- (7) J. Masud et al., *Phys. Rev. Letters*, **58**, (1987), 763;
- (8) R.Bonifacio, C.Pellegrini, L.Narducci, *Opt. Comm.*, **50**, (1984), 373;
- (9) E.T. Scharlemann, *J. Appl. Phys.*, **58**, (1985), 2154.